THE PROTEIN SOCIETY

Aggregation of Trp > Glu point mutants of human gamma-D crystallin provides a model for hereditary or UV-induced cataract

Eugene Serebryany, Takumi Takata, Erika Erickson, Nathaniel Schafheimer, Yongting Wang, and Jonathan A. King*

Department of Biology, Massachusetts Institute of Technology, Cambridge, Massachusetts 02139

Received 8 January 2016; Accepted 10 March 2016
DOI: 10.1002/pro.2924
Published online 14 March 2016 proteinscience.org

Abstract: Numerous mutations and covalent modifications of the highly abundant, long-lived crystallins of the eye lens cause their aggregation leading to progressive opacification of the lens, *cataract*. The nature and biochemical mechanisms of the aggregation process are poorly understood, as neither amyloid nor native-state polymers are commonly found in opaque lenses. The βγ-crystallin fold contains four highly conserved buried tryptophans, which can be oxidized to more hydrophilic products, such as kynurenine, upon UV-B irradiation. We mimicked this class of oxidative damage using Trp→Glu point mutants of human γD-crystallin. Such substitutions may represent a model of UV-induced photodamage—introduction of a charged group into the hydrophobic core generating "denaturation from within." The effects of Trp→Glu substitutions were highly position dependent. While each was destabilizing, only the two located in the bottom of the double Greek key fold—W42E and W130E—yielded robust aggregation of partially unfolded intermediates at 37°C and pH 7. The αB-crystallin chaperone suppressed aggregation of W130E, but not W42E, indicating distinct aggregation pathways from damage in the N-terminal vs C-terminal domain. The W130E aggregates had loosely fibrillar morphology, yet were nonamyloid, noncovalent, showed little surface hydrophobicity, and formed at least 20°C below the melting temperature of the native β-sheets. These features are most consistent with domain-swapped polymerization. Aggregation of partially destabilized crystallins under physiological conditions, as occurs in this class of point mutants, could provide a simple *in vitro* model system for drug discovery and optimization.

Keywords: crystallin; cataract; protein misfolding; protein aggregation; oxidative damage; amyloid; unfolding intermediate

Introduction

Cataract is the major cause of blindness worldwide. It results from aggregation of proteins from the crystallin class and consequent progressive opacification of the eye lens. The likelihood of cataract increases exponentially with age, affecting >50% of those aged 75 or older.[1] Surgery is currently the only effective treatment, although even in the United States, ~10% of patients do not have improved vision after the surgery.[2] In the U.S. alone, about 3 million cataract surgeries are performed every year, at a cost of roughly $6–9 billion, most of it borne by Medicare.[3,4] In the developing world, where the need is greatest, access to surgery is the least and the funding for it is least available. A source of hope is that cataract is a slow disease: a therapy to delay age of onset by 10

Additional Supporting Information may be found in the online version of this article.

Grant sponsor: National Eye Institute; Grant number: #EY015834; Grant sponsor: MIT Biology/Merck.

*Correspondence to: Jonathan A. King; Massachusetts Institute of Technology, 77 Massachusetts Avenue, Cambridge, MA 02139. E-mail: jaking@mit.edu

years would halve the need for surgery and the attendant costs. Recently, genetic studies and high-throughput screens identified the first class of compounds with efficacy in animal models of age-onset cataract, but the mechanisms of their action are not yet understood.[5,6] Here we report that aggregation of oxidation-mimicking mutants of a lens γ-crystallin offers a physiologically relevant *in vitro* model of cataract onset that could facilitate drug screening and development to slow the rate of opacification.

Mature lens fiber cells are enucleated *in utero* or shortly after birth and have no metabolism or protein turnover.[7] Lack of nuclei or mitochondria increases transparency and mitigates production of reactive oxygen species and other damaging byproducts of metabolism. However, the crystallins synthesized *in utero* must maintain their native structure in the face of environmental stresses for a lifetime.[8,9] Crystallins make up >90% of the total protein in this tissue (~400 mg/mL), whose transparency depends on their structural integrity and lack of long-range packing.[10] Crystallins also form a refractive index gradient within the lens, allowing light to be properly focused on the retina.[11] The γ-crystallins are monomeric, while β-crystallins self-associate into dimers or tetramers. Both families have β-sheet-rich duplicated Greek key folds. The α-crystallin chaperones assemble into multimeric complexes in the lens and sequester misfolded or damaged βγ-crystallins to contain aggregation at a stage where the aggregates are too small to scatter significant amounts of light. This passive chaperone capacity decreases with age, even as destabilizing chemical modifications, such as oxidation and deamidation, accumulate.[12–16] The result is progressive increase in light scattering (lens turbidity) due to aggregation. No amyloid or other long-range structure has been found in age-onset cataractous aggregates,[9] but disulfides are common[16–18] as reducing capacity of the lens core cytosol declines during cataractogenesis.[19]

The etiological agents for cataract development are not well-defined. Exposure to a number of agents induces cataract in experimental animals, including selenium, heavy metals, and ionizing radiation.[8,10] The best-defined environmental contributing factors to age of cataract onset in people are tobacco use and exposure to ultraviolet light.[20] Both are thought to act via oxidative damage to the lens crystallins.[15,21]

γD-crystallin is most abundant in the oldest part of the lens, the nucleus, where its concentrations are on the order of 10 mg/mL.[22–24] Studies of its folding and unfolding have revealed a distinctive intermediate with the N-terminal domain unstructured, but the C-terminal domain's structure intact. The domain interface of the C-terminal domain acts as a template for the folding of the N-terminus.[25] Many cases of congenital cataracts are due to mutations in the γD-crystallin gene,[26–30] and we and others have characterized most of the known mutant proteins such as P23T, R14C, W42R, R58H, and V75D.[9,31–35] However, the millions of cases of mature-onset cataract arise without mutations; instead, modified (e.g., oxidatively damaged) forms of the wild-type protein appear to be the precursor.[8,15] Mass spectrometry of surgically removed cataracts has revealed aggregated γD polypeptide chains with oxidative damage.[16,17] Such damage may generate partially unfolded intermediate conformations which polymerize into light-scattering aggregates that either include or overwhelm the passive chaperone content of the lens.[8–10]

Several distinct aggregation pathways have been defined for γD-crystallin *in vitro*.[9] During dilution from denaturant into buffer, partially folded intermediates partition between refolding and aggregation.[36] However, owing to the crystallins' extreme thermodynamic stability, full denaturation is unlikely to ever occur in the lens. Incubation of native protein at pH 3 results in polymerization into well-defined amyloid fibrils.[37–39] However, pH 3 is much more acidic than the physiological pH of lens cytosol, and biophysical investigations have not revealed any amyloid in lenses with the common age-related cataract.[40,41] Cold-induced phase separation ("cold cataract") has been the subject of extensive research, but these reversible native-state aggregates typically dissolve near body temperature.[42,43] Crystallization can also be a source of cataractous light scattering, but only rare surface mutants in γD-crystallin, R58H and R36S, form such "crystal cataracts".[33] The wild-type crystallins (whose name refers to the glassy appearance of the lens) are highly resistant to crystallization. More common are cataractogenic point mutations in the core, leading to partial or transient unfolding of the native structure and consequent polymerization, at physiological pH, concentration, and temperature, into nonamyloid, light-scattering, high-molecular-weight complexes .[34,35,44–46] Remarkably, even when the concentration of such a mutant protein is too low to generate significant aggregation, interaction with the wild-type protein may greatly enhance it.[46] Direct UV-B exposure causes Trp and Cys oxidation and subsequent non-native polymerization,[39,47] likely by a similar pathway as the core mutations. Finally, copper and zinc ions can shift even undamaged, WT γ-crystallins into a non-amyloid aggregated state whose nature remains to be fully characterized.[48]

The duplicated Greek key structure of γ-crystallins (Fig. 1) relies on four conserved Trp residues for thermodynamic stability. When ultraviolet light reaches the lens,[49] it is efficiently absorbed by Trp residues. Though the resulting excited states can be quenched by energy transfer mechanisms, occasionally they result in the opening and oxidation

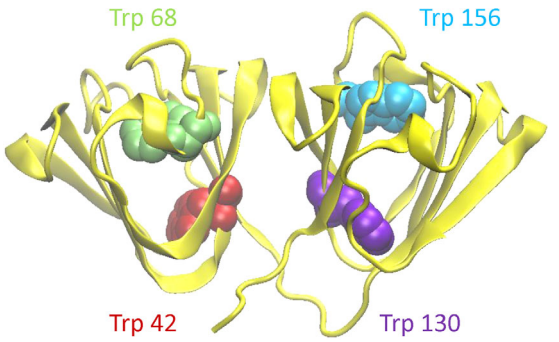

Figure 1. A backbone ribbon representation of the HγD crystal structure (PDB ID 1HK0) (32) showing the four conserved buried Trp residues.

of the indole ring.[39] Oxidation products such as kynurenine form via a charged intermediate.[50] The net effect is that a hydrophobic core residue becomes hydrophilic. To mimic this physiologically relevant class of aggregation, we examined four point mutants of human γD crystallin, in which one of the four Trp residues was replaced by Glu. These substitutions produced aggregation under near-physiological conditions, but in a strongly site-dependent manner.

Inhibitors of crystallin aggregation could retard cataract development. The search for small-molecule aggregation inhibitors has been hampered by the difficulty of recapitulating at high speed *in vitro* the aggregation pathway that proceeds in the eye lens on the time scale of decades. In the case of cataract, the most promising current drug candidates, for example, lanosterol, were found either by genetic analysis or by high-throughput screening, so their mechanism of action is not well understood.[5,6] Here we report a class of mutants of human γD crystallin that shows fast, controllable, non-amyloid aggregation under near-physiological conditions, with aggregate morphology similar to that resulting from direct UV-induced oxidation. We have not yet examined whether specific small molecules can modulate these aggregation reactions. However, because these mutations are at the same sites as are prone to oxidative damage, this class of mutants may be a good model for *in vitro* biochemical and biophysical investigation and offers a simple screening assay for anticataract drugs.

Results

Protein expression and purification

In addition to wild-type HγD, four Trp > Glu point mutants were expressed in M15 *Escherichia coli* for the purpose of this study. They are designated WT,

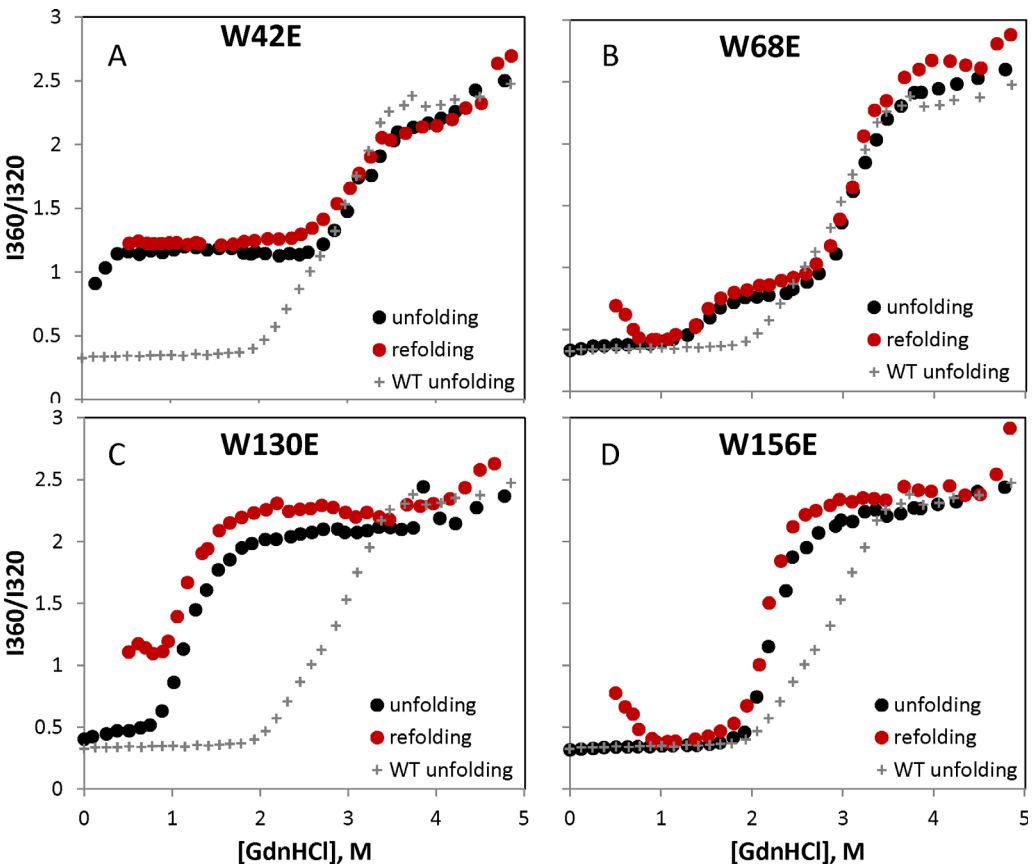

Figure 2. Equilibrium unfolding and refolding curves for the four W > E mutants, with the equilibrium unfolding curve for WT shown on each panel for reference. Deviations in the refolding curves relative to the respective unfolding curves are due to aggregation.

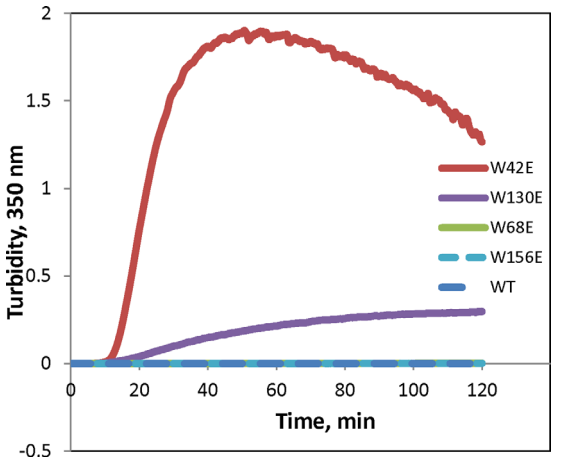

Figure 3. Aggregation of γD at 40.5°C in 10 mM ammonium acetate buffer at pH 7. All proteins are at 1 mg/mL concentration.

W42E, W68E, W130E, and W156E. All constructs carried N-terminal hexahistidine tags (MKHHHH HHQ) for purification. Protein expression following induction by IPTG was carried out overnight at 16°C because expressing the mutants, particularly W130E and W42E, at a higher temperature resulted in little or no soluble protein; instead, the polypeptide chains accumulated as inclusion bodies. For this reason, all steps of the purification were routinely carried out at temperatures not exceeding 16°C. High concentrations of imidazole (~100 mM) resulted in the W42E mutant protein forming aggregates in the fraction tubes overnight following elution from the Ni^{2+} or Co^{2+} column, so dialysis out of imidazole was carried out soon after fraction collection.

Following purification and dialysis, the proteins were stored in 10 mM ammonium acetate, pH 7, at 4–6°C and remained stable for several weeks. If a small amount of precipitate developed during storage, the sample was refiltered to clear it with little loss of protein concentration. The exception was the W42E construct, which, when concentrated to 1.2 mg/mL and stored as usual, was found to aggregate significantly within 2–3 days. For this reason, W42E was stored at a concentration of <0.5 mg/mL and concentrated further only immediately before any experiment requiring high protein concentration.

Yields of soluble W42E and W130E from bacterial preparations were 10–20% of the wild-type yield. The yield of purified protein from the W156E construct was ~50% of wild type. The yield of W68E was comparable to WT.

Folding and stability

All the Trp > Glu mutants showed decreased resistance to chemical denaturation compared to WT, as shown in Figure 2. The curves for the two N-terminal mutants [Fig. 2(A,B)] show the general three-state folding and unfolding pattern found in the βγ-crystallins,[9] where the plateau represents folded C-terminal domain, but unfolded N-terminal domain.[51] In contrast, folding and unfolding of the two C-terminal mutants [Fig. 2(C,D)] is more cooperative, consistent with our previous findings that the domain interface stabilizes or templates the native structure of the N-terminal domain.[25,52] However, intrinsic fluorescence spectra measured under non-denaturing conditions were consistent with native-like structures for all constructs (Supporting Information, Figs. S1 and S2), including the anomalous Trp quenching characteristic of the γ-crystallins.[53]

Equilibrium refolding of the N-terminal domain could not be achieved for the W42E construct due to its high degree of destabilization. In the case of the W130E construct, off-pathway aggregation competed with refolding; the apparent increase in the 360/320 ratio, particularly below 1*M* GdnHCl, is due to light scattering. However, the W42E N-terminal domain was at least partly folded at 37°C without denaturant. In fact, it showed only a modest further decrease in chemical stability relative to the previously reported W42Q and W42R mutants,[35,46] suggesting that in this case, the origin of destabilization lies largely in the hydrophilicity of the substitutions, rather than the negative charge.[54] Every refolded sample formed light scattering aggregates below ~0.5*M* GdnHCl, as reflected in the upturned refolding curve at these low denaturant concentrations.[36] Any apparent hysteresis between the unfolding and refolding scenarios[36] was suppressed by the overnight incubation at 37°C.

Aggregation under near-physiological conditions

At physiological temperatures and pH, wild-type γD-crystallin showed no tendency to aggregate, as shown in Figure 3. We found very different aggregation propensities among the four mutants when incubated at physiological temperature and pH. Representative turbidity traces are shown in Figure 3. W42E had by far the highest aggregation propensity under these conditions; however, W130E aggregation was also strong. On the other hand, W156E showed only modest aggregation, while W68E and the wild-type protein did not aggregate detectably.

The W42E and W130E constructs aggregated in a temperature-dependent manner [Fig. 4(A,B)], with W42E in particular showing a transition between almost undetectable aggregation and fast, robust aggregation with subsequent condensation and settling of the aggregated sample over a range of at most 5°C. This suggests a highly cooperative unfolding transition occurring between 32°C and 37°C in this mutant leading to aggregation. As previously reported,[46] the W42Q mutant, which does not change

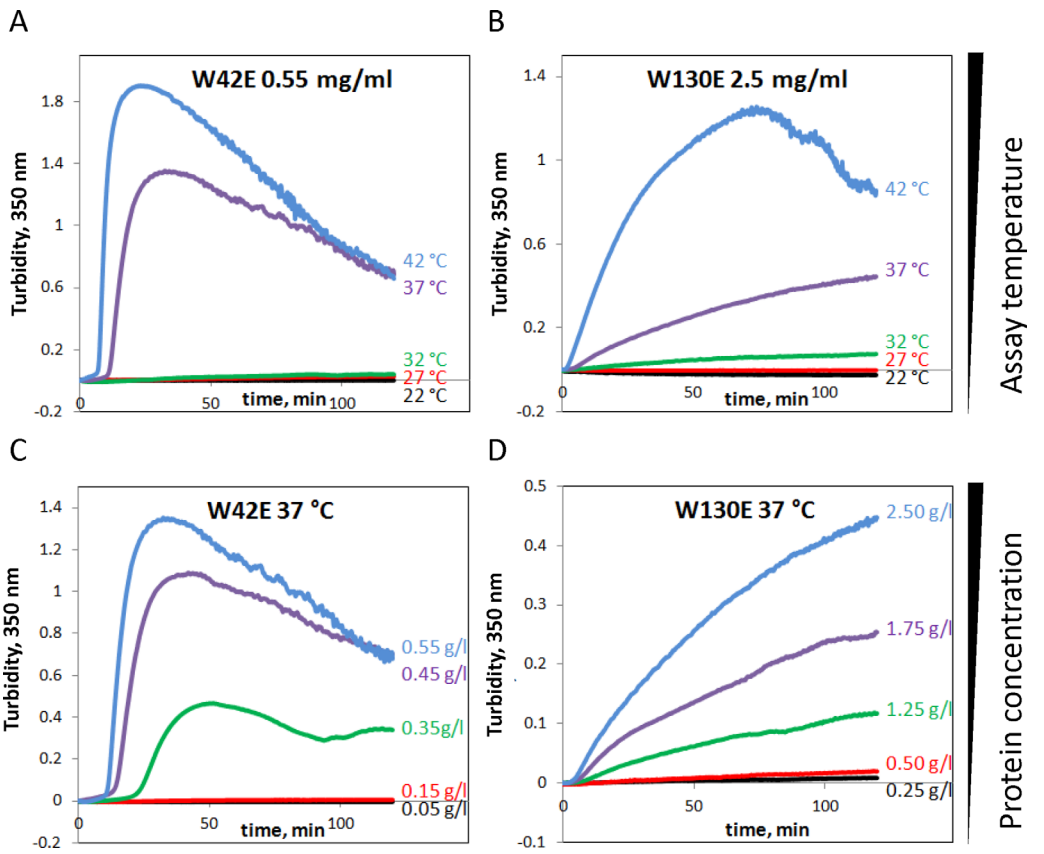

Figure 4. (A,B) Temperature-dependence and (C,D) concentration-dependence of W130E and W42E aggregation.

the charge of the protein, showed a comparably sharp soluble-to-aggregated transition, but the temperature range was ~5°C higher. Compared to W42E, W130E exhibited a broader aggregation temperature range, as well as a weaker concentration dependence of aggregation [Fig. 4(C,D)]. The conformational transition that enables aggregation of W130E may be less cooperative than for W42E. However, it is also possible that the W130E aggregates have a smaller nucleus size than those of W42E.

Amyloid aggregation propensities

It is known that HγD forms amyloid fibrils under acidic conditions,[37–39] and this type of aggregation has been proposed as a possible mechanism for cataractogenesis.[6,55] On the other hand, no amyloid aggregates have been found to date in eye lenses from patients with age-related cataract,[40,41] unlike rare congenital cases.[10,55] Figure 5 shows the differential ability of the four Trp > Glu mutants to form amyloid fibrils, monitored by thioflavin T fluorescence. Remarkably, aggregation propensity at pH 3 did not correlate with aggregation at pH 7. Thus, W68E aggregated more strongly, albeit somewhat less rapidly, than W130E at pH 3, yet W130E, not W68E, showed strong aggregation at pH 7 (Fig. 5).

Comparing two measures of the extent of amyloid aggregation—turbidity and Thioflavin T fluorescence—suggests that the amyloid aggregates themselves are distinct for the various mutants. Thus, W130E exhibited ~4× lower amplitude of turbidity after 30 min than W68E, yet comparable ThT binding. W42E showed no more ThT binding than WT under these conditions. We attribute the late rise in turbidity of the W42E sample, which is not accompanied by any increase in ThT binding, to residual ability of this mutant to form pH7-like aggregates even at pH 3.

We investigated the morphology of the pH 3 aggregates formed by WT and W68E mutants by transmission electron microscopy. As shown in Figure 6, both formed extensive amyloid fibrils even at time zero, which represents the 1.5 min dead time that it takes to extract the sample from the reaction mixture, blot onto the EM sample grid, and allow it to adhere onto the grid. W68E formed abundant, thin amyloid fibril-like aggregates at the early stages of aggregation.

Nonamyloid aggregation of W130E proceeds from a native-like state

Electron micrographs of the heat-induced W130E and W42E aggregates at pH 7 are presented in Figure 7. The morphology of these aggregates, taken after ~2 h at 40.5°C, is distinct from anything observed at pH 3. Both constructs are able to form

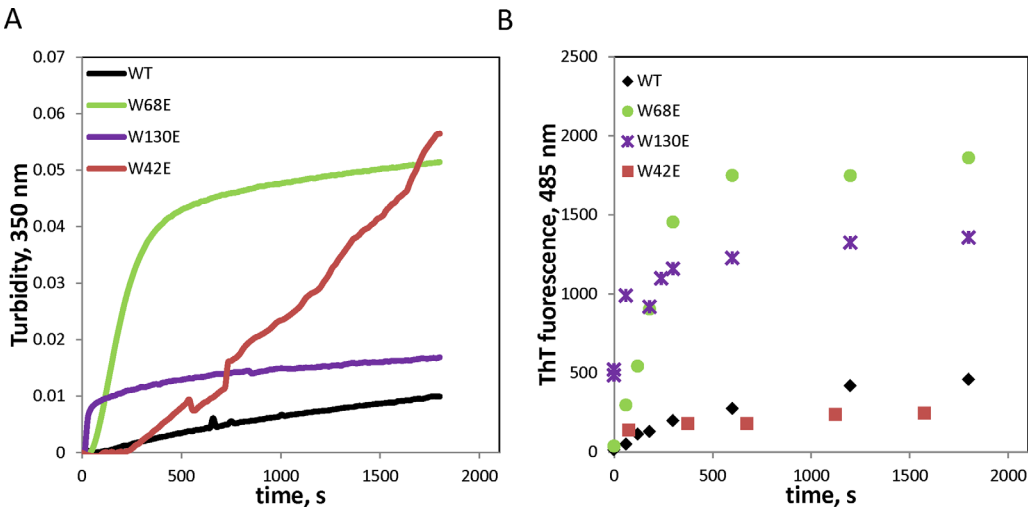

Figure 5. Amyloid aggregation of wild-type and mutant HγD under acidic conditions (pH 3), followed by turbidity (A) and Thioflavin T fluorescence (B).

irregular fibrils; however, extensive condensation into globular particles is also observed in the case of W42E. The appearance of such particles likely explains the declining phase of aggregation observed in Figure 3. They also bear resemblance to the "protein particulates" class of aggregation products examined by Donald et al.[56]

Aggregation of the W130E construct was temperature-sensitive not only for the initiation/nucleation phase but also for the growth phase. As demonstrated in Figure 8(A), dropping the temperature from aggregation-permissive (37°C) to aggregation-restrictive (27°C) after turbidity development was already well underway resulted in a gradual but complete stop in further development of turbidity. When temperature was subsequently raised to 37°C again, the increase in turbidity resumed. However, the pre-existing aggregates appeared unable to seed aggregation of new ones since the slope and lag phase of turbidity development during the second 37°C phase were similar to the first phase.

Similar to the W42Q aggregates we reported previously,[46] the pH 7 aggregates of W130E showed no binding to the amyloid-staining dye Thioflavin T and very little surface hydrophobicity as reported by bis-ANS binding [Fig. 8(B)]. W130E formed amyloids at pH 3 more readily than WT (Fig. 5), consistent with previous observations using UV-catalyzed Trp oxidation.[39] However, dropping the pH from 7 to 3 during the course of the 37°C aggregation reaction resulted in immediate loss of most of the turbidity, followed by the initiation of amyloid aggregation with kinetics comparable to aggregation from natively folded protein. Thus, it appears that the pH 7, 37°C aggregates neither contain abundant amyloid fibers nor efficiently seed their formation. At the same time, the physiological aggregates did not contain disulfide-bridged or other covalently linked oligomers [Fig. 8(C,D)], which leaves some form of domain-swapping as the most plausibly applicable of currently known models of protein aggregation. TEM data showing loosely fibrillar morphology of the aggregates (Fig. 7, *left*) are consistent with this interpretation.

Since W130E aggregation is temperature-sensitive, we measured this construct's thermostability by circular dichroism. The native spectrum of W130E showed at most a very slight difference from WT in the far-UV region [Fig. 9(A)]. Near-UV CD [Fig. 9(B)] showed somewhat less structure than WT, but this difference could also be attributed to the missing Trp residue in W130E. The mutant protein had a melting temperature of 60°C, approximately 22°C lower than the WT protein,[51] but highly stable nonetheless. Most importantly, W130E showed no detectable loss of the native secondary structure in the temperature range of heat-induced aggregation [Fig. 9(C) vs (A)]. We conclude that W130E aggregation requires either a very early unfolding intermediate, such that native secondary structure is not detectably perturbed, or else a very rare and transient conformational excursion, such that the amount of conformationally rearranged protein is undetectably small.

HγD has an extensive surface charge network, which may contribute to its high stability. We therefore tested the effect of added salt on the W130E aggregation kinetics. Addition of 150 m*M* NaCl increased both the speed and the amplitude of aggregation. Adding a divalent cation (Mg^{2+}) did not have any added effect [Fig. 10]. Screening of surface charges may contribute to aggregation *in vivo*.

In the case of W42Q, formation of a non-native disulfide bond is required for aggregation.[46] We examined whether the same is true of W130E. As shown in Figure 11, incubation in a reducing environment significantly diminished the amplitude, though not the kinetics, of aggregation for the W130E mutant.

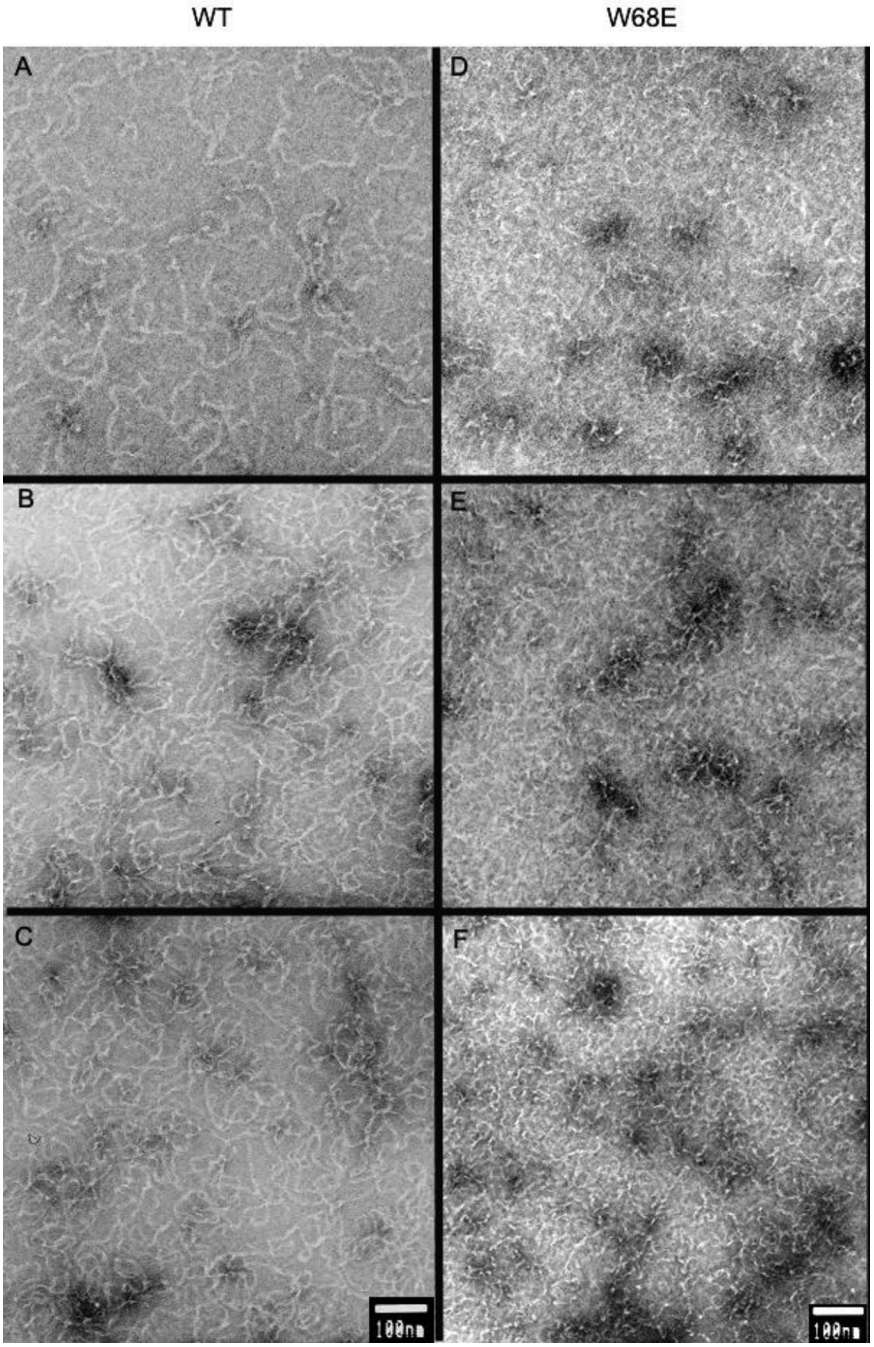

Figure 6. Electron micrographs of acid-induced amyloid fibrils formed by (A–C) WT and (D–F) W68E HγD at different times of aggregation at pH 3. The protein was incubated at 1 mg/mL concentration at 37°C, in 50 mM sodium acetate and 100 mM NaCl, pH 3.0. Aliquotes were taken at (A, D) 0 min, (B, E) 2 min, and (C, F) 5 min after the initiation of aggregation. Scale bars are 100 nm.

Remarkably, the same held true for the construct lacking the N-terminal domain completely [Fig. 11(B)], and the aggregation kinetics of this single-domain mutant were similar to the full-length protein.

Aggregation of W130E, but not W42E, can be suppressed by the αB crystallin chaperone

The chaperone system of the eye lens fiber cells, comprised by the α-crystallins, serves to mitigate the effects of aggregation of other crystallins, thereby delaying the onset of cataract.[8] However, a class of mutants has been found that escapes this chaperone pathway.[57] We therefore studied whether the aggregation of Trp > Glu mutants can be suppressed by the chaperone. As shown in Figure 12, αB was able to suppress aggregation of W130E. In contrast, W42E not only aggregated in the presence of the chaperone but also produced greater turbidity in the presence of the chaperone than in its absence. This experiment cannot determine whether W42E induces aggregation

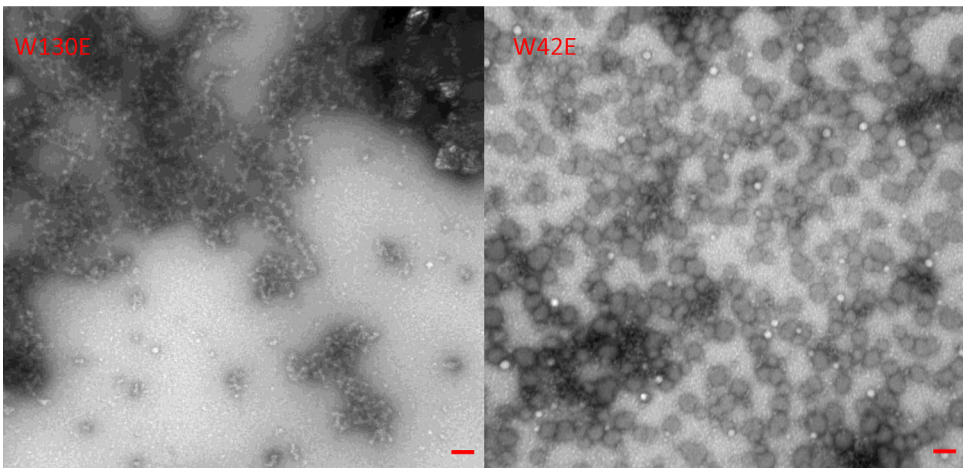

Figure 7. Representative electron micrographs of aggregates formed by W130E and W42E HγD mutants after 2 h at 37°C. Scale bars are 100 nm.

of αB or the interaction with αB enhances the aggregation of W42E by itself. However, the experimental result indicates that aggregation of the W42E mutant cannot be suppressed by the presence of the α-crystallin.

Discussion

Cataract is a widespread but slowly developing disorder, presumably dependent on the kinetics of both initiation and propagation of crystallin aggregation. The detailed molecular mechanism of crystallin aggregation in aging lens remains to be determined. It seems likely, however, that the participating species are covalently modified or damaged *in vivo*. UV light triggers Trp oxidation[39] and the development of cataractogenesis in animal models.[58] Oxidized Trp residues in α-, β-, and γ-crystallins have been found repeatedly in cataractous lenses.[17,59,60] The protective energy-transfer mechanism in γD crystallin depends on pairs of its tryptophan residues,[53] which

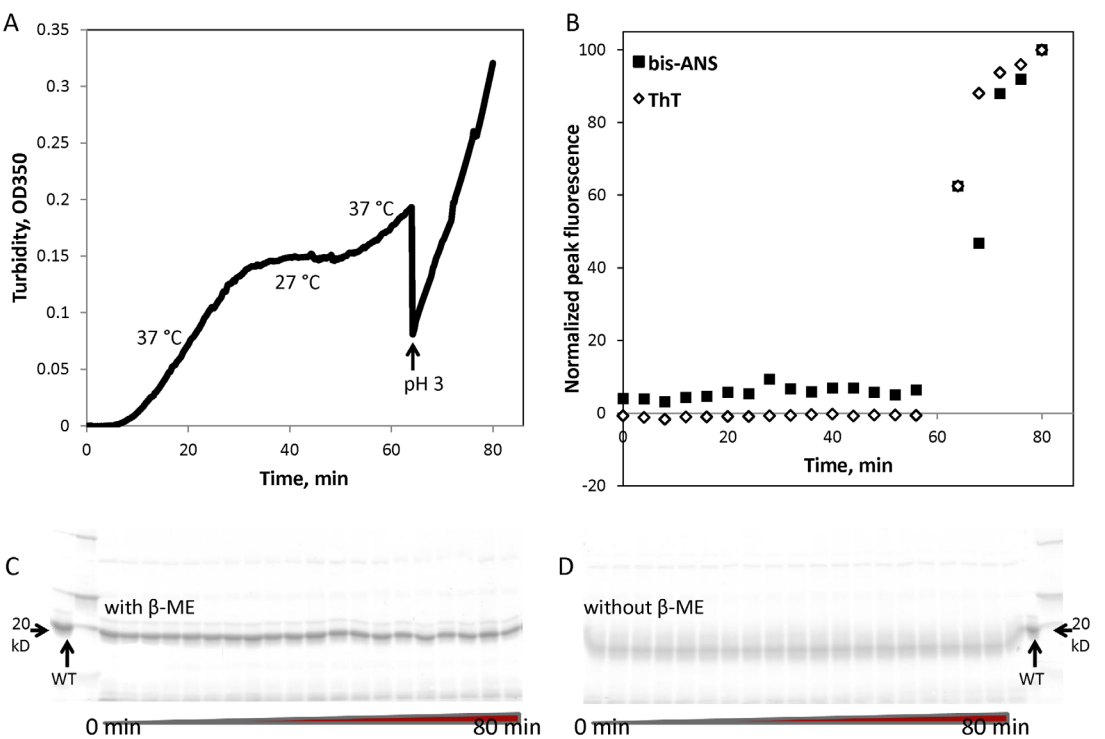

Figure 8. Characterization of heat-induced W130E aggregates. In samples taken from the aggregation timecourse as measured by turbidity (A), staining with thioflavin T and bis-ANS (B) was used to measure amyloid formation and exposure of hydrophobic residues, respectively. SDS-PAGE analysis in the presence (C) or absence (D) of reducing agent (β-mercaptoethanol) did not reveal any covalently linked oligomers. Minor bands that may be backbone cleavage products were observed, but their intensity did not vary during the course of aggregation.

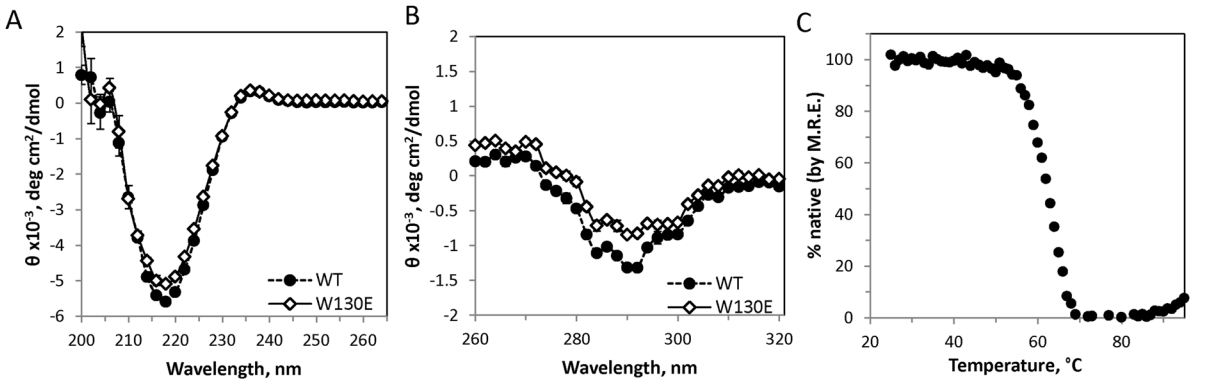

Figure 9. Characterization of W130E structure by circular dichroism. (A) Native CD spectrum of the W130E mutant compared to WT in the far-UV region. (B) Native CD spectra of WT and W130E in the near-UV region. Error bars represent standard error of the mean of 4 measurements. (C) Thermal melt of W130E as monitored by decrease in the 218 nm peak.

also protect the protein against UV-induced aggregation.[47] We report a class of mutants that mimics a possible effect of UV-B exposure on βγ-crystallins, as well as connects genetic and environmental aggregation pathways.[35,46,61] Intrinsic fluorescence (Supporting Information, Figs. S1 and S2) and, for W130E, circular dichroism (Fig. 9) suggest that these mutant proteins are able to fold into the native state. These observations are consistent with the native-like crystal structure of the W42R mutant.[35] However, both W42E and W130E aggregate at physiological temperature and concentration into high-molecular-weight complexes.

The precise pathway of aggregation as a result of the Trp > Glu substitutions will require further study. We have been able to observe that these aggregates are of a nonamyloid nature, and that the physiological aggregation pathway is in competition with amyloid aggregation. The W130E mutation in particular causes little detectable change in secondary or tertiary structure even under temperatures permissive for aggregation. We cannot rule out that the mutations result in increased susceptibility to further chemical modification of the polypeptide, such as oxidation or deamidation; however, any associated conformational change is subtle, without significant loss of overall β-sheet character or change in the fluorescence spectrum. These properties are consistent with polymerization from early unfolding intermediates, such as via domain swapping.

UV irradiation has long been known to contribute to cataract development[8–10,20,49,58] and has been shown directly *in vitro* to induce oxidation of Trp residues in HγD, as well as at least one nearby Cys residue, and open up polymerization pathways.[39,62] Long-timescale molecular dynamics simulations have revealed that Trp oxidation to kynurenine increases water penetration into the hydrophobic core,[63] which may lead to the generation of partially unfolded conformations capable of domain swapping.[64] The oxidation-mimicking W42Q substitution indeed leads to an aggregation pathway without broad denaturation; this pathway requires formation of an internal disulfide bond.[46] This study has revealed that oxidation-mimicking substitution at Trp130 leads to a comparable phenomenon of aggregation with minimal denaturation, whose biochemical and structural properties are broadly consistent with the predictions of the prior simulations. This pathway is redox-sensitive, although unlike W42Q, presence of a reducing agent inhibits it incompletely (Fig. 11). We therefore speculate that UV-induced aggregation is a three-step process. First, oxidative damage creates hydrophilic and/or charged residues within the tight, hydrophobic core of HγD. Second, an oxidation-sensitive conformational rearrangement, perhaps via domain swapping or strand insertion, leads to the formation of dimers and higher-order oligomers and, ultimately, nonamyloid fibrils. Third, prolonged incubation or continued UV

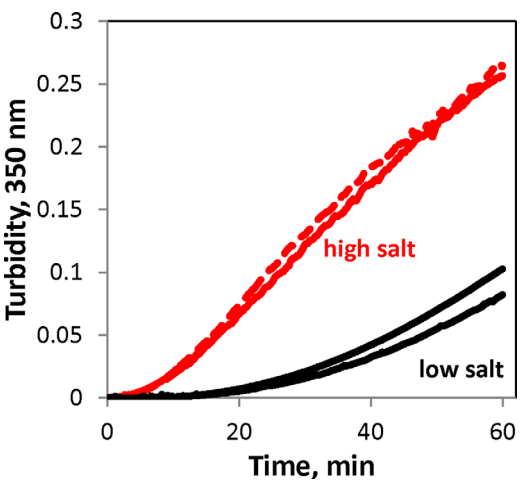

Figure 10. W130E aggregation is sensitive to redox conditions and ionic strength. W130E (1 mg/mL) incubated at 40.5°C in sample buffer alone (10 m*M* ammonium acetate, *black lines*), sample buffer with 150 m*M* NaCl (red solid line), and 150 m*M* NaCl plus 5 m*M* $MgCl_2$ (*red dashed line*).

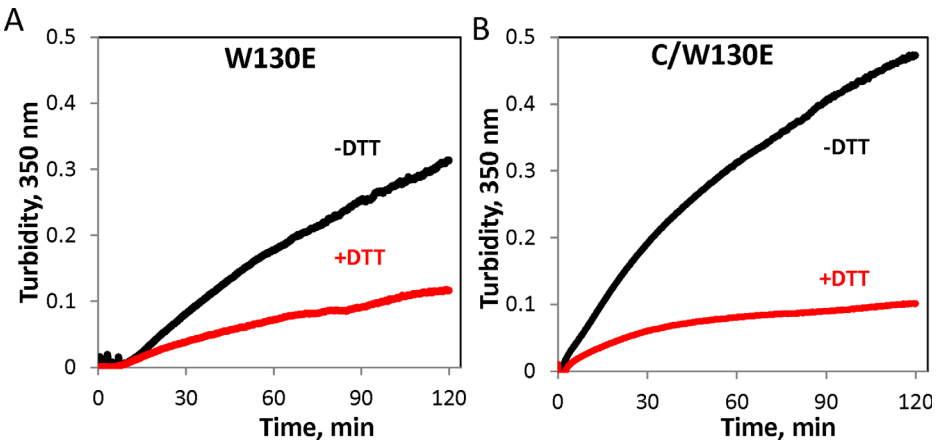

Figure 11. Redox-dependence of aggregation of the W130E mutant and its isolated C-terminal domain. (A) 1.25 mg/mL W130E (59 μM) was incubated at 40.5°C in the presence or absence of 1 mM DTT, (B) Isolated C-terminal domain carrying the W130E mutation incubated at 0.5 mg/mL (47 μM) incubated as in (A).

exposure creates tightly packed aggregates, which may be covalently cross-linked and not easily reversible. The mutations studied here are intended to mimic early stages of cataractogenesis when it is most likely to be reversible.

The observation of strong temperature dependence of propagation [Fig. 8(A)] coupled with relatively weak concentration dependence [Fig. 4(C)] argues that the rate-limiting step in W130E aggregation is unimolecular conformational rearrangement. The fact that the isolated C-terminal domain carrying the W130E mutation exhibits similar aggregation behavior to the full-length W130E suggests this rearrangement occurs within the mutated domain itself. The aggregation process does depend on redox state although not as dramatically as the W42Q mutant.[46] No disulfides have been found in the native state of HγD.[32,65] Since disulfide-bridged oligomers were not found during the course of W130E aggregation [Fig. 8(D)], any potential disulfide involved in stabilizing the misfolded conformation should be internal. Only two Cys residues are located in the HγD C-terminal domain (Cys108 and Cys110), so it is tempting to speculate that the misfolded, aggregation-prone conformation of the W130E mutant protein is stabilized by a disulfide bridge between these two residues. Though the distance between these Cys residues is small (6.6 Å in PDB 1HK0), the protein is notably sensitive to perturbation in this area, since the E107A mutation is known to cause cataract.

Redox homeostasis is lost during the course of lens aging, leading to both intra- and intermolecular disuflide bonds in the lens crystallins, as well as glutathionylation.[16,18,19,66–68] We have previously reported that reducing agents are able to suppress or even completely eliminate aggregation of the W42Q mutant of γD-crystallin.[46] Although the reversal is less dramatic for W130E, strategies designed to restore the redox potential of the lens

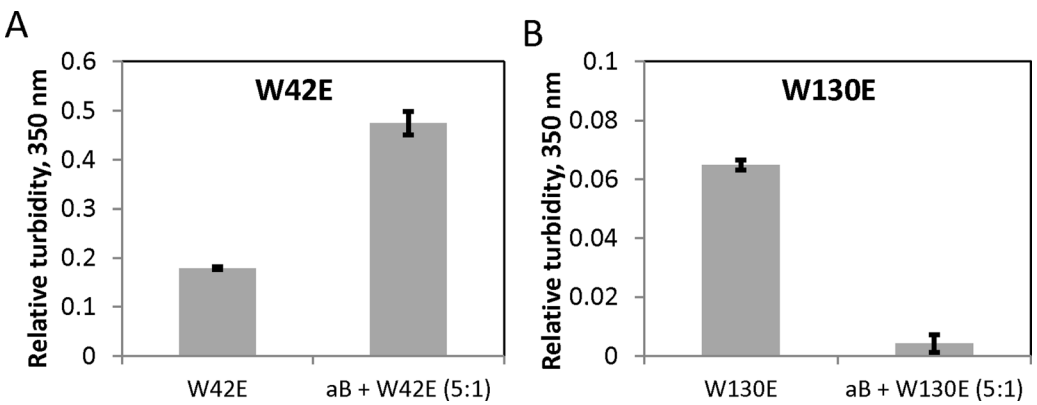

Figure 12. Aggregation of W130E, but not W42E, can be suppressed by fivefold excess of human αB crystallin. (A) Final relative turbidity of W42E incubated for 2 h at 0.125 mg/mL and 40.5°C with or without fivefold excess (0.625 mg/mL) of the chaperone. (B) 1 mg/mL W130E incubated as in (A) with or without fivefold excess (5 mg/mL) of the chaperone. Error bars represent standard errors of the mean of 3 replicates.

are likely to have a beneficial effect in the treatment of cataract.

Despite continuous oxidation over time, cataract onset is delayed *in vivo* by the action of the α-crystallin passive chaperone system present in the lens. Indeed, at least some mutations in the HγD gene appear to exert their cataractogenic effects primarily via altered interactions with the α-crystallins.[69] We have found that aggregation of the W130E mutant is suppressed by αB-crystallin. By contrast, W42E not only escapes suppression by this chaperone but also produces enhanced aggregation when the chaperone is present. Since the V75D mutant is known to also escape from the chaperone,[57] α-crystallin may be unable to suppress aggregation of γD-crystallin with a damaged N-terminal core.

Recent work has shown that lanosterol, which suppresses aggregation of the W42R mutant of HγD *in vitro*, is capable of mitigating cataractogenesis in animal models as well.[5] This connection suggests that oxidation-mimicking Trp substitutions of HγD can be used as one approach for identifying potential drug candidates against crystallin aggregation. Mutants such as those reported here could also be useful for elucidating the biochemical mechanisms of action of such drugs.

Materials and Methods

Protein expression and purification

All HγD constructs were expressed from bacterial IPTG-inducible pQE1 plasmids (Qiagen) and contained an N-terminal His_6 tag (MKHHHHHHQ) for purification. M15 *E. coli* were cultured in Super-Broth (3.2% peptone, 2% yeast extract, 0.5% NaCl) overnight at 16°C following induction with 1 m*M* IPTG. Cells were resuspended in lysis buffer (50 m*M* sodium phosphate, pH 7.4, with or without 10 m*M* imidazole) in the presence of EDTA-free Complete protease inhibitor cocktail (Promega), incubated with ∼5 mg/mL lysozyme and ∼10 μg/mL DNase for 30 min, and lysed by 20–30 30 s bursts of sonication on ice. Lysate was cleared by centrifugation and filtration and applied to either a nickel column or a HisPur (Thermo Fisher) cobalt column for purification (imidazole-free lysis buffer was used with the cobalt column). Columns were washed with 6–50 m*M* imidazole, and the protein was eluted with a linear gradient of elution buffer. Elution buffer contained 300 m*M* NaCl and 250 m*M* imidazole, pH 8 (nickel) or 150 m*M* imidazole, pH 7.4 (cobalt). Imidazole was purchased from Sigma (ReagentPlus®, 99% pure). Size and purity of eluted sample was confirmed by SDS-PAGE, and the best fractions pooled and dialyzed against 3 × 100 volumes of 10 m*M* ammonium acetate, pH 7, for at least 4 h each time. For experiments requiring high concentrations of sample, the dialysate was concentrated using an Amicon centrifugal concentrator unit. All samples were 0.2 μm filtered before storage to remove pre-existing aggregates or other particulate matter.

Equilibrium denaturation and refolding

Equilibrium folding curves were built as described previously.[25] Briefly, protein samples were diluted into varying concentrations of guanidinium chloride and incubated overnight at 37°C. Subsequently, fluorescence spectra were recorded with a Hitachi F-4500 fluorimeter, and the ratio of fluorescence intensities at 360 and 320 nm was used as a reporter of folding state. These wavelengths were chosen because they represent the emission peaks of unfolded and natively folded γD, respectively. Refolding was done by first denaturing the protein in 5 M guanidinium chloride at 37°C for at least 3 h, and then diluting into varying final concentrations of GdnHCl.

Circular dichroism spectroscopy

Far-UV spectra and thermal melts were obtained using a Jasco J-715 spectropolarimeter. All samples were in storage buffer (10 m*M* ammonium acetate). Protein concentration was 0.025 mg/mL. Ellipticity at 218 nm was monitored in the case of thermal melts in order to measure the extent of β-sheet structure. Thermal melting experiments were performed with various rates of heating in order to ascertain that the sample had sufficient equilibration time at each temperature.

Turbidity measurement

Turbidity development during protein aggregation was measured with a UV–Vis spectrophotometer (Varian) equipped with a water bath for temperature control, without stirring. Turbidity as a function of time was recorded at 350 nm. Amyloid aggregation was induced by adding low-pH acetate buffer to a final pH of 3 at 37°C. Nonamyloid aggregation was induced by heat; 40.5°C was typically used to speed up the reaction.

Thioflavin T binding

Samples taken during the course of the heat-induced aggregation reaction were mixed immediately with a solution of 25 μ*M* ThT in 50 m*M* sodium phosphate pH 7 buffer. This buffer was used to efficiently neutralize the pH of the solution prior to measuring ThT fluorescence.

Transmission electron microscopy

Samples from the aggregation reactions were withdrawn and either diluted or placed directly on a glow-discharged carbon-coated formvar-filmed copper grid (Ted Pella), dried, and then stained for 45 s in 1% uranyl acetate. The grid was then dried again and

imaged using a JEOL-1200 transmission electron microscope.

Acknowledgments

The authors thank Cameron Haase-Pettingell for expert technical assistance throughout this study. Deborah Pheasant at the Biophysical Instrumentation Facility for the Study of Complex Macromolecular Systems (NSF-0070319) is gratefully acknowledged. E.S. would like to thank Fanrong Kong for mentorship early in this work. The authors declare no conflicts of interest.

References

1. Klein R, Klein BEK (2013) The prevalence of age-related eye diseases and visual impairment in aging: current estimates. Invest Ophthalmol Vis Sci 54:14, ORSF5–ORSF13.
2. Facts about cataract (2009) National Eye Institute. https://nei.nih.gov/health/cataract/cataract_facts.
3. Frick KD, Gower EW, Kempen JH, Wolff JL (2007) Economic impact of visual impairment and blindness in the United States. Arch Ophthalmol 125:544–550.
4. Tielsch JM, Kempen JH, Congdon N, Friedman DS (2008) Vision probelms in the U.S.: prevalence of adult visual impairment and age-related eye disease in America, p. 22. Prevent Blindness America and the National Eye Institute.
5. Zhao L, Chen XJ, Zhu J, Xi YB, Yang X, Hu LD, Ouyang H, Patel SH, Jin X, Lin DN, Wu F, Flagg K, Cai HM, Li G, Cao GQ, Lin Y, Chen D, Wen C, Chung C, Wang YD, Qiu A, Yeh E, Wang WQ, Hu X, Grob S, Abagyan R, Su ZG, Tjondro HC, Zhao XJ, Luo HR, Hou R, Perry JJP, Gao WW, Kozak I, Granet D, Li YR, Sun XD, Wang J, Zhang LF, Liu YZ, Yan YB, Zhang K (2015) Lanosterol reverses protein aggregation in cataracts. Nature 523:607.
6. Makley LN, McMenimen KA, DeVree BT, Goldman JW, McGlasson BN, Rajagopal P, Dunyak BM, McQuade TJ, Thompson AD, Sunahara R, Klevit RE, Andley UP, Gestwicki JE (2015) Pharmacological chaperone for alpha-crystallin partially restores transparency in cataract models. Science 350:674–677.
7. Wride MA (2011) Lens fibre cell differentiation and organelle loss: many paths lead to clarity. Philos Trans R Soc B Biol Sci 366:1219–1233.
8. Bloemendal H, de Jong W, Jaenicke R, Lubsen NH, Slingsby C, Tardieu A (2004) Ageing and vision: structure, stability and function of lens crystallins. Prog Biophys Mol Biol 86:407–485.
9. Serebryany E, King JA (2014) The βγ-crystallins: native state stability and pathways to aggregation. Prog Biophys Mol Biol 115:32–41.
10. Moreau KL, King JA (2012) Protein misfolding and aggregation in cataract disease and prospects for prevention. Trends Mol Med 18:273–282.
11. Zhao HY, Brown PH, Magone MT, Schuck P (2011) The molecular refractive function of lens gamma-crystallins. J Mol Biol 411:680–699.
12. Michael R, Bron AJ (2011) The ageing lens and cataract: a model of normal and pathological ageing. Philos Trans R Soc B Biol Sci 366:1278–1292.
13. Takata T, Oxford JT, Demeler B, Lampi KJ (2008) Deamidation destabilizes and triggers aggregation of a lens protein, beta A3-crystallin. Protein Sci 17:1565–1575.
14. Lampi KJ, Wilmarth PA, Murray MR, David LL (2014) Lens beta-crystallins: the role of deamidation and related modifications in aging and cataract. Prog Biophys Mol Biol 115:21–31.
15. Truscott RJW (2005) Age-related nuclear cataract - oxidation is the key. Exp Eye Res 80:709–725.
16. Fan X, Zhou S, Wang B, Hom G, Guo M, Li B, Yang J, Vaysburg D, Monnier VM (2015) Evidence of highly conserved β-crystallin disulfidome that can be mimicked by in vitro oxidation in age-related human cataract and glutathione depleted mouse lens. Mol Cell Proteom 14:3211–3223.
17. Hains PG, Truscott RJW (2007) Post-translational modifications in the nuclear region of young, aged, and cataract human lenses. J Proteome Res 6:3935–3943.
18. Hains PG, Truscott RJW (2008) Proteomic analysis of the oxidation of cysteine residues in human age-related nuclear cataract lenses. Biochim Biophys Acta 1784: 1959–1964.
19. Wei M, Xing K-Y, Fan Y-C, Libondi T, Lou MF (2015) Loss of thiol repair systems in human cataractous lenses. Invest Ophthalmol Vis Sci 56:598–605.
20. Robman L, Taylor H (2005) External factors in the development of cataract. Eye 19:1074–1082.
21. Ye J, He JJ, Wang CJ, Wu H, Shi X, Zhang HN, Xie JJ, Lee SY (2012) Smoking and risk of age-related cataract: a meta-analysis. Invest Ophthalmol Vis Sci 53: 3885–3895.
22. Su S, Liu P, Zhang H, Li ZJ, Song Z, Zhang L, Chen S (2011) Proteomic analysis of human age-related nuclear cataracts and normal lens nuclei. Invest Ophthalmol Vis Sci 52:4182–4191.
23. Lampi KJ, Ma ZX, Shih M, Shearer TR, Smith JB, Smith DL, David LL (1997) Sequence analysis of beta A3, beta B3, and beta A4 crystallins completes the identification of the major proteins in young human lens. J Biol Chem 272:2268–2275.
24. Keenan J, Orr DF, Pierscionek BK (2008) Patterns of crystallin distribution in porcine eye lenses. Mol Vis 14:1245–1253.
25. Flaugh SL, Kosinski-Collins MS, King J (2005) Contributions of hydrophobic domain interface interactions to the folding and stability of human gamma D-crystallin. Protein Sci 14:571–581.
26. Pande A, Ghosh KS, Banerjee PR, Pande J (2010) Increase in surface hydrophobicity of the cataract-associated P23T mutant of human gammaD-crystallin is responsible for its dramatically lower, retrograde solubility. Biochemistry 49:6122–6129.
27. Pande A, Annunziata O, Asherie N, Ogun O, Benedek GB, Pande J (2005) Decrease in protein solubility and cataract formation caused by the Pro23 to Thr mutation in human gamma D-crystallin. Biochemistry 44: 2491–2500.
28. Evans P, Wyatt K, Wistow GJ, Bateman OA, Wallace BA, Slingsby C (2004) The P23T cataract mutation causes loss of solubility of folded gammaD-crystallin. J Mol Biol 343:435–444.
29. Santhiya ST, Shyam Manohar M, Rawlley D, Vijayalakshmi P, Namperumalsamy P, Gopinath PM, Löster J, Graw J (2002) Novel mutations in the gamma-crystallin genes cause autosomal dominant congenital cataracts. J Med Genet 39:352–358.
30. Jung J, Byeon IJ, Wang Y, King J, Gronenborn AM (2009) The structure of the cataract-causing P23T mutant of human gammaD-crystallin exhibits distinctive local conformational and dynamic changes. Biochemistry 48:2597–2609.

31. Ji F, Koharudin LMI, Jung J, Gronenborn AM (2013) Crystal structure of the cataract-causing P23T D-crystallin mutant. Proteins 81:1493–1498.
32. Pande A, Gillot D, Pande J (2009) The cataract-associated R14C mutant of human gamma D-crystallin shows a variety of intermolecular disulfide cross-links: a Raman spectroscopic study. Biochemistry 48:4937–4945.
33. Pande A, Pande J, Asherie N, Lomakin A, Ogun O, King J, Benedek GB (2001) Crystal cataracts: human genetic cataract caused by protein crystallization. Proc Natl Acad Sci USA 98:6116–6120.
34. Moreau KL, King JA (2009) Hydrophobic core mutations associated with cataract development in mice destabilize human gamma D-crystallin. J Biol Chem 284:33285–33295.
35. Ji FL, Jung J, Koharudin LMI, Gronenborn AM (2013) The human W42R gamma D-crystallin mutant structure provides a link between congenital and age-related cataracts. J Biol Chem 288:99–109.
36. Kosinski-Collins MS, King J (2003) In vitro unfolding, refolding, and polymerization of human gamma D crystallin, a protein involved in cataract formation. Protein Sci 12:480–490.
37. Papanikolopoulou K, Mills-Henry I, Tho SL, Wang YT, Gross AAR, Kirschner DA, Decatur SM, King J (2008) Formation of amyloid fibrils in vitro by human gamma D-crystallin and its isolated domains. Mol Vis 14:81–89.
38. Wang YT, Petty S, Trojanowski A, Knee K, Goulet D, Mukerji I, King J (2010) Formation of amyloid fibrils in vitro from partially unfolded intermediates of human gamma C-crystallin. Invest Ophthalmol Vis Sci 51:672–678.
39. Moran SD, Zhang TO, Decatur SM, Zanni MT (2013) Amyloid fiber formation in human gamma D-crystallin induced by UV-B photodamage. Biochemistry 52:6169–6181.
40. Truscott RJW, Eye lens proteins in cataract. In: Uversky VN, Fink AL, Eds. (2007) Protein misfolding, aggregation, and conformational diseases. New York: Springer.
41. Metlapally S, Costello MJ, Gilliland KO, Ramamurthy B, Krishna PV, Balasubramanian D, Johnsen S (2008) Analysis of nuclear fiber cell cytoplasmic texture in advanced cataractous lenses from Indian subjects using Debye–Bueche theory. Exp Eye Res 86:434–444.
42. Siezen RJ, Fisch MR, Slingsby C, Benedek GB (1985) Opacification of gamma-crystallin solutions from calf lens in relation to cold cataract formation. Proc Natl Acad Sci USA 82:1701–1705.
43. Liu CW, Lomakin A, Thurston GM, Hayden D, Pande A, Pande J, Ogun O, Asherie N, Benedek GB (1995) Phase-separation in multicomponent aqueous-protein solutions. J Phys Chem 99:454–461.
44. Lee S, Mahler B, Toward J, Jones B, Wyatt K, Dong L, Wistow G, Wu Z (2010) A single destabilizing mutation (F9S) promotes concerted unfolding of an entire globular domain in gamma S-crystallin. J Mol Biol 399:320–330.
45. Mahler B, Doddapaneni K, Kleckner I, Yuan C, Wistow G, Wu Z (2011) Characterization of a transient unfolding intermediate in a core mutant of gamma S-crystallin. J Mol Biol 405:840–850.
46. Serebryany E, King JA (2015) Wild-type human gamma D-crystallin promotes aggregation of its oxidation-mimicking, misfolding-prone W42Q mutant. J Biol Chem 290:11491–11503.
47. Schafheimer N, King J (2013) Tryptophan cluster protects human D-crystallin from ultraviolet radiation-induced photoaggregation in vitro. Photochem Photobiol 89:1106–1115.
48. Quintanar L, Dominguez-Calva JA, Serebryany E, Rivillas-Acevedo L, HaasePettingell C, Amero C, King JA (in press) Copper and zinc ions specifically promote nonamyloid aggregation of the highly stable human γ-D crystallin. ACS Chem Biol.
49. Sliney DH (2002) How light reaches the eye and its components. Intl J Toxicol 21:501–509.
50. Maleknia SD, Wong JWH, Downard KM (2004) Photochemical and electrophysical production of radicals on millisecond timescales to probe the structure, dynamics and interactions of proteins. Photochem Photobiol Sci 3:741–748.
51. Flaugh SL, Mills IA, King J (2006) Glutamine deamidation destabilizes human gamma D-crystallin and lowers the kinetic barrier to unfolding. J Biol Chem 281:30782–30793.
52. Flaugh SL, Kosinski-Collins MS, King J (2005) Interdomain side-chain interactions in human gamma D crystallin influencing folding and stability. Protein Sci 14:2030–2043.
53. Chen J, Callis PR, King J (2009) Mechanism of the very efficient quenching of tryptophan fluorescence in human gamma D- and gamma S-crystallins: the gamma-crystallin fold may have evolved to protect tryptophan residues from ultraviolet photodamage. Biochemistry 48:3708–3716.
54. Denisov VP, Schlessman JL, Garcia-Moreno B, Halle B (2004) Stabilization of internal charges in a protein: water penetration or conformational change? Biophys J 87:3982–3994.
55. Meehan S, Berry Y, Luisi B, Dobson CM, Carver JA, MacPhee CE (2004) Amyloid fibril formation by lens crystallin proteins and its implications for cataract formation. J Biol Chem 279:3413–3419.
56. Krebs MRH, Domike KR, Donald AM (2009) Protein aggregation: more than just fibrils. Biochem Soc Trans 37:682–686.
57. Moreau KL, King JA (2012) Cataract-causing defect of a mutant gamma-crystallin proceeds through an aggregation pathway which bypasses recognition by the alpha-crystallin chaperone. PLoS ONE 7.[PAGE #].
58. Zhang J, Yan H, Lofgren S, Tian XL, Lou MF (2012) Ultraviolet radiation-induced cataract in mice: the effect of age and the potential biochemical mechanism. Invest Ophthalmol Vis Sci 53:7276–7285.
59. MacCoss MJ, McDonald WH, Saraf A, Sadygov R, Clark JM, Tasto JJ, Gould KL, Wolters D, Washburn M, Weiss A, Clark JI, Yates JR (2002) Shotgun identification of protein modifications from protein complexes and lens tissue. Proc Natl Acad Sci USA 99:7900–7905.
60. Finley EL, Dillon J, Crouch RK, Schey KL (1998) Identification of tryptophan oxidation products in bovine alpha-crystallin. Protein Sci 7:2391–2397.
61. Graw J, Jung M, Loster J, Klopp N, Soewarto D, Fella C, Fuchs H, Reis A, Wolf E, Balling R, de Angelis MH (1999) Mutation in the beta A3/A1-crystallin encoding gene Cryba1 causes a dominant cataract in the mouse. Genomics 62:67–73.
62. Schafheimer N, Wang Z, Schey K, King J (2014) Tyrosine/cysteine cluster sensitizing human gamma D-crystallin to ultraviolet radiation-induced photoaggregation in vitro. Biochemistry 53:979–990.
63. Xia Z, Yang Z, Huynh T, King JA, Zhou R (2013) UV-radiation induced disruption of dry-cavities in human gamma D-crystallin results in decreased stability and faster unfolding. Sci Rep 3:1560.
64. Das P, King JA, Zhou R (2011) Aggregation of gamma-crystallins associated with human cataracts via domain

swapping at the C-terminal beta-strands. Proc Natl Acad Sci USA 108:10514–10519.
65. Basak A, Bateman O, Slingsby C, Pande A, Asherie N, Ogun O, Benedek GB, Pande J (2003) High-resolution X-ray crystal structures of human gamma D crystallin (1.25 angstrom) and the R58H mutant (1.15 angstrom) associated with aculeiform cataract. J Mol Biol 328:1137–1147.
66. Friedburg D, Manthey KF (1973) Glutathione and NADP linked enzymes in human senile cataract. Exp Eye Res 15:173–177.
67. Giblin FJ, David LL, Wilmarth PA, Leverenz VR, Simpanya MF (2013) Shotgun proteomic analysis of S-thiolation sites of guinea pig lens nuclear crystallins following oxidative stress in vivo. Mol Vis 19: 267–280.
68. Craghill J, Cronshaw AD, Harding JJ (2004) The identification of a reaction site of glutathione mixed-disulphide formation on gamma S-crystallin in human lens. Biochem J 379:595–600.
69. Banerjee PR, Pande A, Patrosz J, Thurston GM, Pande J (2011) Cataract-associated mutant E107A of human gamma D-crystallin shows increased attraction to alpha-crystallin and enhanced light scattering. Proc Natl Acad Sci USA 108:574–579.